

Bakuchiol Dimers From Psoraleae Fructus That Inhibit Nitric Oxide Production in RAW264.7 Macrophages Cells

Qingxia Xu

Peking University Health Science Centre

Qian Lv

Peking University Health Science Centre

Lu Liu

Peking University Health Science Centre

Yingtao Zhang

Peking University Health Science Centre

Xiuwei Yang (✉ xwyang@bjmu.edu.cn)

Peking University Health Science Centre

Research

Keywords: Psoralea corylifolia, bakuchiol dimers, inhibition of nitric oxide

Posted Date: July 26th, 2021

DOI: <https://doi.org/10.21203/rs.3.rs-706759/v1>

License:  This work is licensed under a Creative Commons Attribution 4.0 International License.

[Read Full License](#)

Abstract

Background: Dried fruit of *Psoralea corylifolia* L. (Psoraleae Fructus) is one of the most popular traditional Chinese medicine with treatment for nephritis, spermatorrhea, pollakiuria, asthma, and various inflammatory diseases. Bakuchiol is main meroterpenoid with bioactive diversity from Psoraleae Fructus.

Methods: Various column chromatography methods were used for isolation experiment. Structures and configurations of these compounds were determined by spectroscopic methods and single-crystal X-ray diffraction. Their inhibition on nitric oxide (NO) production in lipopolysaccharide (LPS)-stimulated RAW264.7 macrophages were evaluated by the Griess reaction.

Results: Twelve unrepresented bakuchiol dimmers, bisbakuchiols M–U (1–9) and bisbakuchiol ethers A–C (10–12), along with five known compounds (13–17), were isolated from the fruits of *Psoralea corylifolia* L. Compounds 1–3 and 10–14 exhibited inhibitory activities against LPS-induced NO production in RAW264.7 macrophages, and the inhibition of compound 1 ($IC_{50} = 11.47 \pm 1.57 \mu\text{M}$) was equal to that of L-NIL ($IC_{50} = 10.29 \pm 1.10 \mu\text{M}$) as a positive control.

Conclusions: Seventeen bakuchiol dimers (1–17), including 12 undescribed dimers and 5 known compounds, were isolated. Bisbakuchiol M (1), whose other bakuchiol unit was cyclized to form a 6/6/5 tricyclic system, was a new skeleton compound. Some compounds exhibited NO inhibition activities and the inhibition of compound 1 was equal to that of L-NIL, a positive control. These findings suggested that Psoraleae Fructus provided natural anti-inflammatory constituents and bisbakuchiol M had the potential to be novel NO inhibitor.

1. Background

The higher plant, *Psoralea corylifolia* L. (*Cullen corylifolia* (L) Mefik) is an annual herb and belongs to family Leguminosae distributed in China, India, Malay peninsula, and Indonesia [1]. Dried fruit of *P. corylifolia* (Psoraleae Fructus) is one of the most popular traditional Chinese medicine (TCM) and officially listed in Chinese Pharmacopoeia [2], and it is also a natural food additive [3]. It has been used for the treatment of nephritis, spermatorrhea, pollakiuria, asthma, and various inflammatory diseases [4]. Psoraleae Fructus contains approximately 110 compounds including coumarins, flavonoids, meroterpenoids, and benzofurans [5]. Among these, meroterpenoids are considered to be the one of characteristic and active components [6, 7].

Bakuchiol is main meroterpenoid that consists of a side chain (3-ethenyl-3,7-dimethyl-1,6-octadienyl) and a *p*-disubstituted benzene ring. Structural changes including oxidation, dehydration reduction, condensation and alkylation, occur in the side chain and benzene ring, which increases structural and bioactive diversities of meroterpenoid constituents. According to a review of predecessors' researches, 22 meroterpenoids and 12 bakuchiol dimers were found from the plant [5, 8–10]. In our previous researches [11, 12], fourteen meroterpenoids and seventeen heterodimers of bakuchiol have been reported and their cytotoxicity were evaluated. Further investigation on the cyclohexane extract brought about twelve

unpresented bakuchiol dimmers, bisbakuchiols M–U (1–9) and bisbakuchiol ethers A–C (10–12), along with five known compounds (13–17).

Compound 1 was a new skeleton possessing an undescribed 6/6/5 tricyclic-4,11-dione system deriving from 2,5-dihydroxybakuchiol intramolecular cyclization, and its' plausible biosynthetic pathway was proposed. Moreover, compound 2 was a biphenyl dimer constructed by C₃–C₃' bond and compounds 10–12 were rare heterodimers of bakuchiol and terpenoid. Herein the structure elucidation of these compounds and evaluation of their ability to inhibit nitric oxide (NO) production in lipopolysaccharide (LPS)-stimulated RAW264.7 macrophages were discussed.

2. Materials And Methods

2.1. General experimental procedures

Infrared data were recorded on a Thermo Nicolet Nexus 470 FT-IR spectrometer. Ultraviolet data were acquired on a Mapada UV-6100 double beam spectrophotometer. HRESIMS data were collected using a Waters Xevo G2 QTOF spectrometer. NMR spectra were recorded on a Bruker AVANCE III HD 400 NMR spectrometer. Optical rotations were measured on a Rudolph Autopol IV automatic polarimeter. X-ray data were collected by a Rigaku Micromax-003 X-ray single-crystal diffractometer with CuK α radiation. Open column chromatography (CC) was performed by packing silica gel (200–300 mesh, Marine Chemical Ltd., Qingdao, China), Sephadex LH-20 gel (Pharmacia Biotek, Denmark). Thin layer chromatography (TLC) was carried out on silica gel GF254 plates (Merck, Darmstadt, Germany) with 10% H₂SO₄ in 95% ethanol followed by heating. Reversed phase semi-preparative HPLC (RP-SP-HPLC) was accomplished using an LC3000 system (Beijing Innovation Technology Co., Ltd), equipped with a phenomenon C₁₈ column (21.2 mm \times 250 mm, 5 μ m). Cells were cultured in Sanyo MCO-15 AC carbon dioxide (CO₂) incubator (Sanyo Electric Co., Ltd., Osaka, Japan).

HPLC grade solvents, methanol (MeOH) and acetonitrile (MeCN), were purchased from Fisher Scientific (Pittsburgh, PA, USA) and solvents, petroleum ether (PE), cyclohexane (cHE), ethyl acetate (EtOAc), chloroform (CHCl₃) and normal-butanol (BuOH) for column chromatography purchased from Beijing Chemical Works (Beijing, China). Dulbecco's modified Eagle's medium (DMEM), fetal bovine serum (FBS), trypsin, penicillin-streptomycin solution, phosphate buffered saline were obtained from Gibco® (Life Technologies Inc., Grand Island, NY, USA). 3-(4,5-Dimethyl-2-thiazolyl)-2,5-diphenyl-2H-tetrazolium bromide (MTT), lipopolysaccharide (LPS), Griess reagent, dimethylsulfoxide (DMSO), and *L*-N⁶-(1-iminoethyl)-lysine (L-NIL) were obtained from Sigma-Aldrich (St. Louis, MO, USA). The murine macrophage cell line RAW264.7 was obtained from the Cell Bank of the Chinese Academy of Sciences (Shanghai, China).

2.2. Plant material

The mature fruits of *Psoralea corylifolia* L. were harvested from Yunnan province of People's Republic of China (GPS coordinates:23°32'N, 99°23'E) in October 2016, and authenticated by Prof. Xiu-Wei Yang of

the School of Pharmaceutical Sciences, Peking University. A voucher specimen (accession number: BGZ201610) of the fruits was deposited at the State Key Laboratory of Natural Medicines and Biomimetic Drugs of Peking University.

2.3. Extraction and isolation

The dried mature fruits powder (47.9 kg) was extracted with 70% aqueous ethanol under reflux. After extracted for three times (first 479 kg for 2 h, and then 384 kg for 2 h two times), the crude extract (8.2 kg, yield 17.12%) was obtained. And then, part of the residue (6.0 kg) was suspended in H₂O (8 L) and extracted with cHE (8 L × 8), EtOAc (8 L × 8) and *n*-butanol (BuOH, 8 L × 8) successively and afforded corresponding extract for 1.2 kg, 2.2 kg and 0.7 kg. The cHE extract (1.0 kg) was fractionated by silica gel column (SGC, 140 mm i.d. × 800 mm) with gradient eluent (PE-EtOAc, 5:1, 3:1, 1:1, 2:3, 1:3, 0:1, v/v) to give 26 fractions (Fr. A–Z). The Fr. B (27.2 g) was separated by SGC (55 mm i.d. × 650 mm) with a step gradient eluent of PE-EtOAc (100: 1, 50: 1, 25: 1, 7: 1, 5: 1, 3:1, 1: 1, 1:3, 0:1, v/v) to afford 15 subfractions (Fr. B-1–Fr. B-15). Fr. B-8 (2.1 g) was separated by reversed-phase column (RPC), eluted with MeCN-H₂O (40:60 to 100:0, v/v), to give 13 subfractions. Fr. B-8-5 was purified by SP-RP-HPLC (MeCN-H₂O, 95:5, v/v), to yield compound **10** (5 mg, t_R = 85 min). The Fr. C (136 g) was separated by SGC (120 mm i.d. × 600 mm) with a step gradient eluent of PE-EtOAc (100: 1, 50: 1, 20: 1, 15: 1, 10: 1, 5:1, 5: 2, 1:1, 0:1, v/v) to afford 16 subfractions (Fr. C-1–Fr. C-16). Fr. C-4-7 was separated by Sephadex LH-20 column (SC) and purified by SP-RP-HPLC (MeCN-H₂O, 93:7, v/v), to yield compound **1** (230 mg, t_R = 45 min) and **11** (60 mg, t_R = 80 min). Fr. C-5 (20 g) was separated by RPC, eluted with MeOH-H₂O (80:20 to 100:0, v/v), to give 9 subfractions. Fr.C-5-9 was separated by SC and purified by SP-RP-HPLC (MeCN-H₂O, 93:7, v/v), to yield compound **12** (34 mg, t_R = 71 min). By SP-RP-HPLC (MeCN-H₂O, 90:10, v/v) and preparative TLC (PE-CHCl₃, 10:1, v/v), compound **2** (104 mg, t_R = 252 min) was obtained from Fr. C-11 (2.1 g). The Fr. D (335 g) was separated by SGC (140 mm i.d. × 800 mm) with a step gradient eluent of PE-CHCl₃ (100: 1, 50: 1, 20: 1, 10: 1, 5: 1, 4:1, 3: 1, 2: 1, 1: 1, 1:3, 0:100, v/v) to afford 14 subfractions (Fr. D-1–Fr. D-14). Fr. D-4 (20.7 g) was separated by RPC, eluted with MeOH-H₂O (45:55 to 100:0, v/v), to give 13 subfractions. Fr. D-4-12 was purified by SP-RP-HPLC (MeOH-H₂O, 93:7, v/v), to yield compounds **8** (15 mg, t_R = 131 min) and **9** (28 mg, t_R = 136 min). By SP-RP-HPLC (MeCN-H₂O, 90:10, v/v), Fr. D-7(1.7 g) was separated to yield compounds **3** (5 mg, t_R = 95 min) and **4** (2 mg, t_R = 87 min). The Fr. D-9 (37 g) was separated by SGC (55 mm i.d. × 650 mm) with a step gradient eluent of PE-CHCl₃ (100: 1, 50: 1, 20: 1, 10: 1, 9: 1, 8:1, 7: 1, 6: 1, 5: 1, 4:1, 3:1, 1:1, 1:3, 0:1, v/v) to afford 28 subfractions. By SP-RP-HPLC (MeOH-H₂O, 92:8, v/v), Fr. D-9-13 was separated to yield compounds **5** (11 mg, t_R = 77 min), **6** (9 mg, t_R = 100 min) and **7** (19 mg, t_R = 110 min). Fr. D-9-25 was purified by SP-RP-HPLC (MeOH-H₂O, 92:8, v/v), to give compounds **13** (18 mg, t_R = 86 min) and **14** (25 mg, t_R = 92 min). Fr. D-9-26 was purified by SP-RP-HPLC (MeOH-H₂O, 92:8, v/v), to give compound **15** (15 mg, t_R = 76 min). Fr. D-11 (19.2 g) was separated by RPC, eluted with MeOH-H₂O (45:55 to 100:0, v/v), to give 27 subfractions. The Fr. D-11-25 (5.9 g) was separated by SGC (35 mm i.d. × 500 mm) with a step gradient eluent of PE-CHCl₃ (8:1, 7: 1, 6: 1, 5: 1, 4:1, 3:1, 1:1, 1:3, 0:100, v/v) to afford 18

subfractions. By SP-RP-HPLC (MeOH-H₂O, 75:25, v/v), Fr. D-11-25-12 was separated to yield compounds **16** (14 mg, *t_R* = 286 min) and **17** (15 mg, *t_R* = 328 min).

Bisbakuchiol M (**1**). Brown-red needle crystals; mp 114–116 °C; [*a*]_D²⁵ + 50.0 (*c* 0.1, MeOH); UV (MeOH) λ_{max} (log ϵ): 204 (4.85), 258 (4.80), 386 (4.28) nm; IR (KBr) ν_{max} 3315, 2967, 2930, 1692, 1609, 1582, 1504, 1385, 1358, 1255, 1035 cm⁻¹; ¹H NMR (CDCl₃, 400 MHz), see Table 1; ¹³C NMR (CDCl₃, 100 MHz), see Table 2; HRESIMS *m/z* 537.3004 [M + H]⁺ (calcd for C₃₆H₄₁O₄, 537.3005).

Bisbakuchiol N (**2**). Yellow oils; [*a*]_D²⁵ + 20.0 (*c* 0.1, MeOH); UV (MeOH) λ_{max} (log ϵ): 203 (4.41), 253 (4.44) nm; IR (KBr) ν_{max} 3319, 2966, 2924, 1703, 1633, 1603, 1496, 1409, 1373, 1231, 969 cm⁻¹; ¹H NMR (CDCl₃, 400 MHz), see Table 1; ¹³C NMR (CDCl₃, 100 MHz), see Table 2; HRESIMS *m/z* 511.3573 [M + H]⁺ (calcd for C₃₆H₄₇O₂, 511.3576).

Bisbakuchiol O (**3**). Yellowish oils; [*a*]_D²⁵ + 30.0 (*c* 0.1, MeOH); UV (MeOH) λ_{max} (log ϵ): 203 (4.57), 267 (4.33) nm; IR (KBr) ν_{max} 3373, 2962, 2926, 1704, 1604, 1507, 1454, 1372, 1238, 1172, 1007 cm⁻¹; ¹H NMR (CDCl₃, 400 MHz), see Table 1; ¹³C NMR (CDCl₃, 100 MHz), see Table 2; HRESIMS *m/z* 555.3468 [M + HCOO]⁻ (calcd for C₃₇H₄₇O₄, 555.3474).

Bisbakuchiol P (**4**). Yellowish oils; [*a*]_D²⁵ - 26.7 (*c* 0.1, MeOH); UV (MeOH) λ_{max} (log ϵ): 202 (4.61), 267 (4.32) nm; IR (KBr) ν_{max} 3381, 2968, 2927, 1703, 1604, 1507, 1452, 1375, 1240, 1172, 1000 cm⁻¹; ¹H NMR (CDCl₃, 400 MHz), see Table 1; ¹³C NMR (CDCl₃, 100 MHz), see Table 2; HRESIMS *m/z* 509.3417 [M - H]⁻ (calcd for C₃₆H₄₅O₂, 509.3420).

Bisbakuchiol Q (**5**). Yellowish oils; [*a*]_D²⁵ + 70.0 (*c* 0.1, MeOH); UV (MeOH) λ_{max} (log ϵ): 202 (4.76), 264 (4.55) nm; IR (KBr) ν_{max} 3370, 2964, 2921, 1704, 1607, 1507, 1459, 1370, 1238, 1171, 1099 cm⁻¹; ¹H NMR (CDCl₃, 400 MHz), see Table 1; ¹³C NMR (CDCl₃, 100 MHz), see Table 2; HRESIMS *m/z* 525.3364 [M - H]⁻ (calcd for C₃₆H₄₅O₃, 525.3369).

Bisbakuchiol R (**6**). White amorphous powder; [*a*]_D²⁵ + 70.0 (*c* 0.1, MeOH); UV (MeOH) λ_{max} (log ϵ): 203 (4.57), 260 (4.35) nm; IR (KBr) ν_{max} 3372, 2967, 2924, 1704, 1613, 1506, 1451, 1365, 1253, 1143, 1094 cm⁻¹; ¹H NMR (CDCl₃, 400 MHz), see Table 1; ¹³C NMR (CDCl₃, 100 MHz), see Table 2; HRESIMS *m/z* 603.3676 [M + HCOO]⁻ (calcd for C₃₈H₅₁O₆, 603.3686).

Bisbakuchiol S (**7**). White amorphous powders; [*a*]_D²⁵ + 60.0 (*c* 0.1, MeOH); UV (MeOH) λ_{max} (log ϵ): 204 (4.42), 260 (4.32) nm; IR (KBr) ν_{max} 3373, 2968, 2925, 1705, 1614, 1506, 1450, 1364, 1235, 1143, 1082 cm⁻¹; ¹H NMR (CDCl₃, 400 MHz), see Table 1; ¹³C NMR (CDCl₃, 100 MHz), see Table 2; HRESIMS *m/z* 557.3635 [M - H]⁻ (calcd for C₃₇H₄₉O₄, 557.3631).

Bisbakuchiol T (**8**). Yellowish oils; $[\alpha]_{25}^D - 20.0$ (c 0.1, MeOH); UV (MeOH) λ_{\max} ($\log \epsilon$): 202 (4.68), 222 (4.57), 262 (4.33) nm; IR (KBr) ν_{\max} 3395, 2967, 2921, 1702, 1588, 1507, 1450, 1375, 1267, 1171, 1010 cm^{-1} ; ^1H NMR (CDCl_3 , 400 MHz), see Table 1; ^{13}C NMR (CDCl_3 , 100 MHz), see Table 2; HRESIMS m/z 525.3367 $[\text{M} - \text{H}]^-$ (calcd for $\text{C}_{36}\text{H}_{45}\text{O}_3$, 525.3369).

Bisbakuchiol U (**9**). Yellowish oils; $[\alpha]_{25}^D + 20.0$ (c 0.1, MeOH); UV (MeOH) λ_{\max} ($\log \epsilon$): 202 (4.63), 265 (4.21) nm; IR (KBr) ν_{\max} 3387, 2966, 2922, 1703, 1587, 1507, 1451, 1374, 1267, 1171, 1009 cm^{-1} ; ^1H NMR (CDCl_3 , 400 MHz), see Table 1; ^{13}C NMR (CDCl_3 , 100 MHz), see Table 2; HRESIMS m/z 525.3371 $[\text{M} - \text{H}]^-$ (calcd for $\text{C}_{36}\text{H}_{45}\text{O}_3$, 525.3369).

Bakuchiol ether A (**10**). Yellowish oils; $[\alpha]_{25}^D + 10.0$ (c 0.1, MeOH); UV (MeOH) λ_{\max} ($\log \epsilon$): 204(4.26), 260(4.15) nm; IR (KBr) ν_{\max} 3424, 2969, 2929, 1712, 1603, 1505, 1453, 1369, 1224, 1136, 913 cm^{-1} ; ^1H NMR (CDCl_3 , 400 MHz), see Table 3; ^{13}C NMR (CDCl_3 , 100 MHz), see Table 3; HRESIMS m/z 445.3080 $[\text{M} + \text{Na}]^+$ (calcd for $\text{C}_{29}\text{H}_{42}\text{O}_2\text{Na}$, 445.3083).

Bakuchiol ether B (**11**). Yellowish oils; $[\alpha]_{25}^D + 20.0$ (c 0.1, MeOH); UV (MeOH) λ_{\max} ($\log \epsilon$): 206(4.50), 265(4.45) nm; IR (KBr) ν_{\max} 3420, 2926, 2864, 1715, 1606, 1507, 1463, 1364, 1245, 1173, 969 cm^{-1} ; ^1H NMR (CDCl_3 , 400 MHz), see Table 3; ^{13}C NMR (CDCl_3 , 100 MHz), see Table 3; HRESIMS m/z 477.3713 $[\text{M} + \text{H}]^+$ (calcd for $\text{C}_{33}\text{H}_{49}\text{O}_2$, 477.3733).

Bakuchiol ether C (**12**). Yellowish oils; $[\alpha]_{25}^D + 30.0$ (c 0.1, MeOH); UV (MeOH) λ_{\max} ($\log \epsilon$): 206(4.46), 263(4.42) nm; IR (KBr) ν_{\max} 3420, 2952, 2927, 1710, 1604, 1505, 1452, 1375, 1241, 1171, 967 cm^{-1} ; ^1H NMR (CDCl_3 , 400 MHz), see Table 3; ^{13}C NMR (CDCl_3 , 100 MHz), see Table 3; HRESIMS m/z 475.3532 $[\text{M} - \text{H}]^-$ (calcd for $\text{C}_{33}\text{H}_{47}\text{O}_2$, 475.3576).

2.4. X-ray Crystallographic Analysis

The X-ray crystallographic experiments were carried out on a XtaLAB Synergy R, HyPix diffractometer with $\text{CuK}\alpha$ radiation. Crystallographic data (No. CCDC 1993852) of **1** have been deposited at the Cambridge Crystallographic Data Center.

Crystallographic data of **1**: $\text{C}_{72}\text{H}_{80}\text{O}_8$, $M = 1073.36$, $a = 13.2661(2)$ Å, $b = 14.3761(2)$ Å, $c = 31.3617(5)$ Å, $\alpha = 90^\circ$, $\beta = 90^\circ$, $\gamma = 90^\circ$, $V = 5981.13(18)$ Å³, $T = 100$ K, space group $P2_12_12_1$, $Z = 4$, μ (Cu K α) = 0.599 mm^{-1} , Crystal size = 0.99 × 0.4 × 0.02 mm^3 , 2θ range for data collection = 8.344 to 139.15826790°, 26790 reflections measured, 10867 independent reflections ($R_{\text{int}} = 0.0431$, $R_{\text{sigma}} = 0.0446$). The final R_1 value was 0.0475 ($I > 2\sigma(I)$). The final wR (F^2) value was 0.1153. Flack parameter = -0.02 (12).

2.5. ECD calculations

The calculation was performed by the Gaussian 16 software. Conformation analysis were proceeded with the MMFF94s molecular mechanics force field. Optimization of the stable conformers with a Boltzmann

distribution over 1% was conducted by time-dependent density functional theory (TD-DFT) at the Cam-B3LYP/6-31 + G(d, p) level for compounds **8** and **9**, with the CPCM model in MeOH. The ECD data was analysed by SpecDis v1.71 with the half-bandwidth no more than 0.3 eV. The final ECD spectra were obtained based on the Boltzmann-calculated contribution of each conformer.

2.6. Inhibition assay on NO production

RAW264.7 cells were maintained in DMEM containing 10% FBS, in a constant humidity atmosphere of 5% CO₂ and 95% air at 37°C. The cells were cultivated at a density of 3 × 10⁵ cells/mL for 24 h in 96-well culture plates. And then, the cells were stimulated with LPS (1 µg/mL) and treated with various concentrations (1.5625–50 µM) of assay compounds. After exposure to the compounds for 24 h, MTT (20 µL, 5mg/mL) was added to each well [13]. Four hours later, 100 µL of lysis solution (40 g SDS, 20 mL isopropanol, 0.4 mL concentrated HCl and 400 mL ddH₂O) was added to dissolve the formazan crystals. Absorbances at 490 nm were measured after 10h by a Multiskan MK3 Automated Microplate Reader (Thermo-Labsystems, Franklin, MA, USA).

The RAW264.7 cells were grown at a density of 3 × 10⁵ cells/mL in 96-well culture plates. After 24 h, the cells were stimulated with LPS (1 µg/mL) and treated with various non-cytotoxic concentrations of assay compounds. And then, the cell culture supernatant (100 µL) was collected and reacted with the same volume of Griess reagent (100 µL) for 15 min at room temperature [14]. The absorbance was determined at 540 nm. The experiments were performed in parallel for three times, and L-NIL was used as a positive control. IC₅₀ (half maximal inhibitory concentration) value of each compound was defined as the concentration (µM) that caused 50% inhibition of NO production. The IC₅₀ values were calculated by the software SPSS 16.0 (SPSS Inc., Chicago, IL, USA).

3. Results

Phytochemical investigation on cHE fraction of 70% ethanol extract of Psoraleae Fructus resulted in twelve unrepresented bakuchiol dimmers (**1–12**) and five known compounds (**13–17**) (Fig. 1). Structures of these new compounds were assigned by NMR spectra and single crystal X-ray diffraction. Compounds **1–3**, **6–9**, and **13–17** could be detected from ultrasonic extraction of Psoraleae Fructus by LC/MS analysis, suggesting that these compounds were natural products (Fig. S94).

Compound **1** was obtained as brown-red needle crystals (MeOH) with mp 114–116 °C. It had the molecular formula C₃₆H₄₀O₄, as established by HRESIMS at *m/z* 537.3004 [M + H]⁺ (calcd for 609.3216). Compared with the NMR data (Tables 1 and 2) of bakuchiol [15], a side chain (3-ethenyl-3,7-dimethyl-1,6-octadienyl) and a *p*-disubstituted benzene ring in **1** were identical to that of bakuchiol. The ¹H NMR data of an another side chain of compound **1** exhibited three methyl groups at δ_H 1.78 (3H, s), 1.78 (3H, s) and 1.44 (3H, s); a vinyl group at δ_H 5.87 (1H, dd, *J* = 10.6, 7.5 Hz, H-17'), 5.19 (1H, br d, *J* = 3.9 Hz, Ha-18'), and 5.16 (1H, br d, *J* = 10.6, Hb-18'); two trisubstituted olefinic protons at δ_H 5.68 (1H, s) and 7.43 (1H, s); and one methylene group at δ_H 2.60 (1H, d, *J* = 18.7 Hz, Ha-10') and 2.46 (1H, d, *J* = 18.7 Hz, Hb-10'). The

presence of an α,β -unsaturated ketone group was revealed by the band at 1692 cm^{-1} in its IR spectrum, which was confirmed by the resonance at $\delta_{\text{C}} 180.4(\text{s})$ in its ^{13}C NMR spectrum. Comparison of the ^{13}C NMR spectrum of **1** with those of bakuchiol, the chemical shifts of C-3 and C-5 were shifted downfield to $\delta_{\text{C}} 121.4$, suggesting that this substituted group was connected to C-4 of bakuchiol moiety by an ether linkage. The full assignment of ^1H and ^{13}C NMR resonances was supported by $^1\text{H}-^1\text{H}$ COSY, DEPT, HSQC and HMBC spectral analyses. The X-ray structure was shown in Fig. 2 and confirmed the absolute configuration of $9S,9'S$ for **1**. Thus, the structure of **1** was as shown in Fig. 1 and named bisbakuchiol M.

The plausible biosynthetic pathway of bisbakuchiol M was proposed (Fig. 3). Hydroxylation reactions occurred at the positions of C-2 and C-5 in bakuchiol to form M1. Once the 4-hydroxyl group in M1 lost a proton to generate M2-1, migrations of the double bond would start. The double bond at C-7 and C-8 would attack C-12 to form a five-membered ring, along with the generation of carbanion at C-13 (M2-2). Subsequently, the carbanion at C-13 attacked C-6 to form six-membered ring (M2-3). The proton at C-6 left, which was accompanied by electron migrations of negative ion of oxygen to produce ketone carbonyl (M3). And then, the α -proton of double bond at C-8 was easily to be hydroxylated to generate M4. The elimination reaction would follow to the generation of M5. Similarly, the hydroxylation occurred at C-11 (M6). Subsequently, 11-hydroxyl group would be oxidized to ketone carbonyl (M7). Finally, M7 and bakuchiol were condensed to produce bisbakuchiol M.

Compound **2** was isolated as yellow oils. The resonances in the ^1H NMR spectrum [δ_{H} 7.26, d, 2.4 Hz; 6.97, d, 8.5 Hz; and 7.34, dd, 8.5, 2.4 Hz] in **2** suggested clearly the 2,5,6-nature of the aromatic protons. Compared with the NMR data of bakuchiol, a side chain (3-ethenyl-3,7-dimethyl-1,6-octadienyl) in **2** was identical to that of bakuchiol. Compound **2** had a molecular formula $\text{C}_{36}\text{H}_{46}\text{O}_2$ on the basis of the HRESIMS ion at m/z 511.3573 $[\text{M} + \text{H}]^+$. Consequently, the structure of compound **2** was unambiguously identified as a dimer comprising two bakuchiol units by a C-C linkage, and it was given the trivial name bisbakuchiol N.

Compound **3** was isolated as yellowish oils with $[\alpha]_{\text{D}}^{25} + 30.0$, and possessed a molecular formula of $\text{C}_{36}\text{H}_{46}\text{O}_2$ by the HRESIMS ion at m/z 555.3468 $[\text{M} + \text{HCOO}]^-$. The IR spectrum of **3** showed absorption bands at 3373, 1604, 1507, 1454, 1238, 1007 cm^{-1} ascribable to hydroxyl group and ether functions and aromatic ring. Compared with the NMR data of bakuchiol, a side chain (3-ethenyl-3,7-dimethyl-1,6-octadienyl) and a *p*-disubstituted benzene ring in **3** were identical to that of bakuchiol, together with a set of remaining NMR signals, which were very similar to those of psoracorylifol F characterized from the fruits of *P. corylifolia* [16]. However, the correlations between H-17' at δ_{H} 6.43 and H-7' at δ_{H} 2.89 were observed, which indicated that H-7' was α -oriented. The large coupling constant ($J = 11.7\text{ Hz}$) of H-7' and H-12' indicated a *trans* configuration of the two methine protons. Likewise, the configuration of H-8' was confirmed β -oriented on the basis of the large coupling constant ($J = 10.6\text{ Hz}$). Thus, the configuration was assigned as $7'S,8'S,9'S,12'S$ from the occurrence of ($9S$)-bakuchiol only from nature [17, 18]. Furthermore, the HMBC cross-peaks of H-8' at δ_{H} 4.06 with aromatic C-4 at δ_{C} 159.7 correlation indicated

that C-8' was connected to C-4 of bakuchiol moiety by an ether linkage (Fig. 4). According to the above data, the structure of compound **3**, named bisbakuchiol O, was established as shown in Fig. 1.

Compound **4** was also isolated as yellowish oils with $[\alpha]_{25}^D -26.7$ (c 0.1, MeOH), and possessed the same molecular formula, $C_{36}H_{46}O_3$, as **3** according to the HRESIMS m/z 509.3417 $[M - H]^-$. Similarly, NMR data (Tables 1 and 2) for compound **4** was comparable to those of compound **3**. Compared with compound **3**, H-7' at δ_H 2.96 (1H, br dd, $J = 11.7, 10.5$ Hz) displayed a NOE correlation with 16'-CH₃ at δ_H 1.30 (1H, s), indicating that they were cofacial, and H-7' was assigned in a β -configuration. And the large coupling constants ($J = 11.7, 10.5$ Hz) indicated that H-8' and H-12' were α -oriented. As a result, the configuration was confirmed as 7'*R*,8'*R*,9'*S*,12'*R*. According to the above data, compound **4** was a dimer, whose C-8' of psoracorylifol F was connected to aromatic C-4 of bakuchiol moiety by an ether linkage (Fig. 4). Thus, the structure of compound **4**, named bisbakuchiol P, was established as shown in Fig. 1.

Compound **5** possessed the molecular formula of $C_{36}H_{46}O_3$ as determined by its HRESIMS ion at m/z 525.3364 $[M - H]^-$. Combined with NMR data, a set of bakuchiol unit signals except for downfield shift to δ_C 157.0 for C-4 and a set of psoracorylifol A unit signals [19] except for downfield shift to δ_C 79.9 for C-7' were observed. In the HMBC spectrum of **5** (Fig. 4), a psoracorylifol A unit located at C-4 of the bakuchiol unit was verified by correlations from H-7' at δ_H 5.17 to C-4 at δ_C 157. These features permitted assignment of the planar structure of compound **5** as shown in Fig. 1. In the NOESY spectrum (Fig. 5), correlations between H-7' at δ_H 5.17 and CH₃-16' β at δ_H 1.10, H-8' at δ_H 3.46 and CH₃-16' β , indicated that H-7' and H-8' were β -oriented. Whereas H-12' at δ_H 4.58 was α -oriented, which was verified by correlations from H-8' and CH₃-15' at δ_H 1.35. Thus, the absolute structure of compound **5**, named bisbakuchiol Q, was established as 9*S*,7'*S*,8'*S*,9'*S*,12'*S*.

Compound **6** was isolated as white amorphous powders, and possessed the molecular formula of $C_{37}H_{50}O_4$ as deduced by HREIMS m/z 603.3676 $[M + HCOO]^-$. Combined with the various NMR experiments, a set of bakuchiol unit signals except for downfield shift to δ_C 123.7 for C-3, C-5 and a set of psoracorylifol A unit signals except for downfield shift to δ_C 82.9 for C-7' and δ_C 82.0 for C-13' were observed. In the HMBC experiment (Fig. 4), a characteristic methoxyl group at δ_H 3.04 (3H, s) correlated with C-7' enabled us to attach this methoxyl group to the C-7'. In NMR spectra of **6**, the signals of an *exo*-methylene of psoracorylifol A unit had disappeared, while a new signal for characteristic methyl group at δ_H 0.49 (3H, s) and an oxygenated quaternary carbon at δ_C 82.0 had appeared. Combined with the downfield shift of C-3 and C-5 of bakuchiol unit, it was obvious that two units were attached together by C₄-O-C₁₃'. In the NOESY spectrum (Fig. 5), correlations between H-7' at δ_H 4.18 and CH₃-16' β at δ_H 1.10, H-8' at δ_H 3.96 and CH₃-16' β , indicated that they were cofacial and were β -oriented. Similarly, correlations from H-8' and CH₃-15' at δ_H 0.82 supported that H-12' at δ_H 3.14 was α -oriented. Finally, the structural assignment of **6** was assigned as 9*S*,7'*S*,8'*S*,9'*S*,12'*S*, and compound **6** was named bisbakuchiol R.

Compound **7** was isolated as white amorphous powders, and possessed the same molecular formula, $C_{37}H_{50}O_4$, as **6** according to the HRESIMS data (m/z 557.3635 $[M - H]^-$). Its 1D NMR pattern was highly

overlapped to that of compound **6**, indicating their same planar structure. In the NOESY spectrum (Fig. 5), correlations between H-7' at δ_{H} 4.30, H-8' at δ_{H} 3.54, and CH₃-16' β at δ_{H} 1.17 indicated that they were cofacial and were β -oriented. Meanwhile, correlations from H-8' and H-12' at δ_{H} 4.08 suggested β -orientation of H-12'. Finally, the structural assignment of **7** was 9*S*,7'*S*,8'*S*,9'*S*,12'*R* as shown in Fig. 1 and compound **7** was named bisbakuchiol.

Table 1
¹H NMR (400 MHz, CDCl₃; δ_H, *J* in Hz) data for compounds 1–9.

Position	1	2	3	4	5	6	7	8	9
1									
2	7.42 (d, 8.6)	7.26 (d, 2.4)	7.00 (d, 8.6)	6.96 (d, 8.7)	7.17 (d, 8.4)	7.19 (d, 8.6)	7.21 (d, 8.5)	6.93 (br s)	6.92 (br s)
3	7.04 (d, 8.6)		6.43 (d, 8.6)	6.36 (d, 8.7)	6.72 (d, 8.4)	6.72 (d, 8.6)	6.79 (d, 8.5)		
4									
5	7.04 (d, 8.6)	6.97 (d, 8.5)	6.43 (d, 8.6)	6.36 (d, 8.7)	6.72 (d, 8.4)	6.72 (d, 8.6)	6.79 (d, 8.5)	6.86, overlapped	6.85, overlapped
6	7.42 (d, 8.6)	7.34 (dd, 8.5, 2.4)	7.00 (d, 8.6)	6.96 (d, 8.7)	7.17 (d, 8.4)	7.19 (d, 8.6)	7.21 (d, 8.5)	6.85, overlapped	6.85, overlapped
7	6.33 (d, 16.2)	6.29 (d, 16.3)	6.13 (d,16.3)	6.11 (d, 16.2)	6.18 (d, 16.2)	6.25 (d, 16.2)	6.26 (d, 16.2)	6.19 (d, 16.2)	6.19 (d, 16.2)
8	6.20 (d, 16.2)	6.11 (d, 16.3)	5.95 (d, 16.3)	5.93 (d, 16.2)	5.99 (d, 16.2)	6.08 (d, 16.2)	6.09 (d, 16.2)	6.03 (d, 16.2)	6.03 (d, 16.2)
9									
10	1.53 (m)	1.50 (m)	1.45 (m)	1.45 (m)	1.46 (m)	1.49 (m)	1.50 (m)	1.46 (m)	1.46 (m)
11	1.98 (m)	1.96 (m)	1.92 (m)	1.91 (m)	1.93 (m)	1.94 (m)	1.95 (m)	1.93 (m)	1.93 (m)
12	5.12 (m)	5.10 (m)	5.09 (br t, 7.1)	5.08 (br t, 6.9)	5.08 (br t, 7.3)	5.10 (br t, 7.3)	5.10 (br t, 7.3)	5.09 (br t)	5.09 (br t)
13									
14	1.60 (s)	1.58 (s)	1.57 (s)	1.66 (s)	1.56 (s)	1.58 (s)	1.58 (s)	1.57 (s)	1.57 (s)
15	1.68 (s)	1.67 (s)	1.66 (s)	1.56 (s)	1.66 (s)	1.67 (s)	1.67 (s)	1.67 (s)	1.67 (s)
16	1.23 (s)	1.20 (s)	1.15 (s)	1.14 (s)	1.15 (s)	1.19 (s)	1.19 (s)	1.17 (s)	1.17 (s)

Position	1	2	3	4	5	6	7	8	9
17	5.87 (dd, 17.6, 11.0)	5.88 (dd, 17.4, 10.7)	5.84 (dd, 17.2, 10.8)	5.83 (dd, 17.2, 10.8)	5.84 (dd, 17.7, 10.7)	5.87 (dd, 17.5, 10.9)	5.87 (dd, 17.5, 10.8)	5.85 (dd, 17.6, 10.7)	5.85 (dd, 17.6, 10.7)
18a	5.04 (dd, 17.6, 1.3)	5.02 (dd, 17.4, 1.4)	4.97 (dd, 17.2, 1.4)	4.97 (dd, 17.2, 1.4)	4.96 (dd, 17.7, 1.3)	5.01 (dd, 17.5, 1.3)	5.01 (dd, 17.5, 1.3)	5.01 (dd, 10.7, 1.3)	5.01 (dd, 10.7, 1.3)
18b	5.08 (dd, 11.0, 1.3)	5.04 (dd, 10.7, 1.4)	5.00 (dd, 10.8, 1.4)	5.00 (dd, 10.8, 1.4)	5.00 (dd, 10.7, 1.3)	5.03 (dd, 10.9, 1.3)	5.02 (dd, 10.8, 1.3)	4.99 (dd, 17.6, 1.3)	4.99 (dd, 17.6, 1.3)
1'									
2'		7.26 (d, 2.4)	7.00 (d, 8.6)	7.01 (d, 8.7)	7.16 (d, 8.7)	7.24 (d, 8.5)	7.18 (d, 8.4)	7.19 (br d, 8.6)	7.16 (br d, 8.6)
3'	5.68 (s)		6.56 (d, 8.6)	6.56 (d, 8.7)	6.71 (d, 8.7)	6.77 (d, 8.5)	6.74 (d, 8.4)	6.73 (br d, 8.6)	6.77 (br d, 8.6)
4'									
5'		6.97 (d, 8.5)	6.56 (d, 8.6)	6.56 (d, 8.7)	6.71 (d, 8.7)	6.77 (d, 8.5)	6.74 (d, 8.4)	6.73 (br d, 8.6)	6.77 (br d, 8.6)
6'		7.34 (dd, 8.5, 2.4)	7.00 (d, 8.6)	7.01 (d, 8.7)	7.16 (d, 8.7)	7.24 (d, 8.5)	7.18 (d, 8.4)	7.19 (br d, 8.6)	7.16 (br d, 8.6)
7'	7.43 (s)	6.29 (d, 16.3)	2.89 (br dd, 11.7, 10.6)	2.96 (br dd, 11.7, 10.5)	5.17 (d, 2.2)	4.18 (d, 8.7)	4.30 (d, 3.0)	4.80 (d, 7.3)	4.91 (d, 6.1)
8'		6.11 (d, 16.3)	4.06 (d, 10.6)	4.05 (d, 10.5)	3.46 (d, 2.2)	3.96 (d, 8.7)	3.54 (d, 3.0)	3.97 (d, 7.3)	4.04 (d, 6.1)
9'									
10'a	2.60 (d, 18.7)	1.50 (m)	1.98 (m)	1.72 (m)	1.86 (m)	1.76 (m)	2.32 (m)	1.76 (m)	1.55 (m)
10'b	2.46(d, 18.7)		1.56 (m)	1.64 (m)	1.62 (m)	1.76 (m)	1.49 (m)	1.30 (m)	1.44 (m)

Position	1	2	3	4	5	6	7	8	9
11'a		1.96 (m)	1.79 (dd, 12.3, 3.3),	1.70 (dd, 11.8, 3.5)	1.93 (m)	1.74 (m)	1.85 (m)	1.93(m)	1.83 (m)
11'b		1.96 (m)	1.55 (dd, 12.3, 3.3)	1.60 (dd, 11.8, 3.5)	1.88 (m)	1.74 (m)	1.85 (m)	1.82 (m)	1.83 (m)
12'		5.10 (m)	2.53 (dt, 12.3, 3.3)	2.47 (dt, 11.8, 3.5)	4.58 (m)	3.14 (m)	4.08 (dd, 3.0)	5.06 (m)	5.03 (m)
13'									
14'	1.78 (s)	1.58 (s)	4.57 (br s), 4.54 (br s)	4.58 (br s) 4.56 (br s)	4.95 (d, 1.3) 4.91 (d, 1.3)	0.82 (s)	1.11 (s)	1.58 (s)	1.57 (s)
15'	1.78 (s)	1.67 (s)	1.51 (s)	1.56 (s)	1.35 (s)	0.49 (s)	1.09 (s)	1.66 (s)	1.67 (s)
16'	1.44 (s)	1.20 (s)	1.04 (s)	1.30 (s)	1.10 (s)	1.10 (s)	1.17 (s)	0.62 (s)	1.07 (s)
17'	5.87 (dd, 10.6, 7.5)	5.88 (dd, 17.4, 10.7)	6.43 (dd, 17.2, 10.8)	5.83 (dd, 17.2, 10.8)	6.46 (dd, 17.7, 10.9)	6.15 (dd, 17.5, 10.9)	6.02 (dd, 17.5, 10.8)	5.84 (dd, 17.4, 10.8)	5.48 (dd, 17.7, 11.0)
18'a	5.19 (br d, 3.9)	5.02 (dd, 17.4, 1.4)	5.20 (dd, 17.2, 1.4)	5.20 (dd, 17.2, 1.4)	4.81 (d, 1.6)	5.14 (dd, 17.5, 1.3)	5.05 (dd, 17.5, 1.3)		
18'b	5.16 (br d, 10.6)	5.04 (dd, 10.7, 1.4)	5.29 (dd, 10.8, 1.4)	5.29 (dd, 10.8, 1.4)	4.85 (d, 1.6)	4.99 (dd, 10.9, 1.3)	5.02 (dd, 10.8, 1.3)		
OCH3						3.04 (s)	3.16 (s)		

Table 2
¹³C NMR (100 MHz, CDCl₃) data for compounds 1–9.

Position	1	2	3	4	5	6	7	8	9
1	136.2, C	131.6, C	130.3, C	129.9, C	130.5, C	132.7, C	132.8, C	131.3, C	131.4, C
2	127.8, CH	123.4, CH	126.6, CH	126.4, CH	126.9, CH	126.3, CH	126.4, CH	113.7, CH	113.9, CH
3	121.4, CH	128.9, C	115.9, CH	116.3, CH	115.2, CH	123.7, CH	124.0, CH	143.7, C	143.4, C
4	152.0, C	152.1, C	159.7, C	159.4, C	157.0, C	155.3, C	154.3, C	143.0, C	143.0, C
5	121.4, CH	116.7, CH	115.9, CH	116.3, CH	115.2, CH	123.7, CH	124.0, CH	116.5, CH	116.4, CH
6	127.8, CH	127.6, CH	126.6, CH	126.4, CH	126.9, CH	126.3, CH	126.4, CH	119.5, CH	119.5, CH
7	125.9, CH	126.1, CH	126.6, CH	126.7, CH	126.5, CH	126.6, CH	126.7, CH	126.5, CH	126.6, CH
8	138.9, CH	136.7, CH	135.3, CH	135.1, CH	135.7, CH	136.5, CH	136.5, CH	136.1, CH	136.1, CH
9	42.7, C	42.6, C	42.4, C	42.4, C	42.5, C	42.5, C	42.5, C	42.5, C	42.5, C
10	41.2, CH ₂	41.2, CH ₂	41.3, CH ₂	41.3, CH ₂	41.2, CH ₂	41.2, CH ₂	41.2, CH ₂	41.3, CH ₂	41.3, CH ₂
11	23.2, CH ₂	23.2, CH ₂	23.3, CH ₂	23.2, CH ₂	23.5, CH ₂	23.2, CH ₂	23.2, CH ₂	23.2, CH ₂	23.2, CH ₂
12	124.6, CH	124.7, CH	124.8, CH	124.8, CH	124.8, CH	124.8, CH	124.8, CH	124.8, CH	124.8, CH
13	131.4, C	131.3, C	131.2, C	131.2, C	131.2, C	131.3, C	131.3, C	131.5, C	131.4, C
14	17.7, CH ₃	17.6, CH ₃	17.6, CH ₃	17.6, CH ₃	17.6, CH ₃	17.6, CH ₃	17.6, CH ₃	17.6, CH ₃	17.6, CH ₃
15	25.7, CH ₃	25.7, CH ₃	25.7, CH ₃	25.7, CH ₃	25.7, CH ₃	25.7, CH ₃	25.7, CH ₃	25.7, CH ₃	25.7, CH ₃
16	23.2, CH ₃	23.3, CH ₃	23.3, CH ₃	23.3, CH ₃	23.4, CH ₃	23.3, CH ₃	23.3, CH ₃	23.4, CH ₃	23.4, CH ₃
17	145.5, CH	145.8, CH	146.0, CH	146.0, CH	146.0, CH	145.9, CH	145.9, CH	145.9, CH	145.9, CH

Position	1	2	3	4	5	6	7	8	9
18	112.3, CH ₂	112.0, CH ₂	111.7, CH ₂	111.7, CH ₂	111.8, CH ₂	111.9, CH ₂	111.9, CH ₂	113.9, CH ₂	111.8, CH ₂
1'	131.6, C	131.6, C	133.3, C	133.3, C	131.9, C	131.5, C	132.4, C	130.4, C	130.4, C
2'	163.8, C	123.4, CH	126.6, CH	129.9, CH	128.0, CH	130.6, CH	128.9, CH	129.8, CH	129.6, CH
3'	104.5, CH	128.9, C	114.7, CH	114.7, CH	115.7, CH	114.8, CH	114.8, CH	115.4, CH	115.2, CH
4'	180.4, C	152.1, C	153.6, C	153.6, C	154.8, C	154.1, C	154.7, C	156.1, C	156.0, C
5'	144.8, C	116.7, CH	114.7, CH	114.7, CH	115.7, CH	114.8, CH	114.8, CH	115.4, CH	115.2, CH
6'	146.8, C	127.6, CH	126.6, CH	129.9, CH	128.0, CH	130.6, CH	128.9, CH	129.8, CH	129.6, CH
7'	126.6, CH	126.1, CH	49.0, CH	48.1, CH	79.9, CH	82.9, CH	84.8, CH	77.4, CH	76.4, CH
8'	122.7, C	136.7, CH	89.1, CH	87.8, CH	83.1, CH	80.5, CH	83.8, CH	81.8, CH	81.4, CH
9'	43.5, C	42.6, C	43.5, C	42.5, C	39.0, C	38.6, C	39.2, C	43.0, C	43.6, C
10'	51.4, CH ₂	41.2, CH ₂	36.6, CH ₂	35.5, CH ₂	34.0, CH ₂	32.8, CH ₂	30.7, CH ₂	38.3, CH ₂	38.8, CH ₂
11'	204.2, C	23.2, CH ₂	27.9, CH ₂	27.2, CH ₂	23.2, CH ₂	20.5, CH ₂	20.3, CH ₂	22.2, CH ₂	22.2, CH ₂
12'	163.0, C	124.7, CH	51.0, CH	50.7, CH	76.0, CH	76.3, CH	78.4, CH	124.5, CH	124.6, CH
13'	37.7, C	131.3, C	147.0, C	146.9, C	144.6, C	82.0, C	82.7, C	131.6, C	131.3, C
14'	22.3, CH ₃	17.6, CH	111.9, CH ₂	112.0, CH ₂	111.5, CH ₂	20.9, CH ₃	24.2, CH ₃	17.5, CH ₃	17.5, CH ₃
15'	22.5, CH ₃	25.7, CH ₃	19.2, CH ₃	19.3, CH ₃	19.3, CH ₃	23.4, CH ₃	21.9, CH ₃	25.7, CH ₃	25.7, CH ₃
16'	23.9, CH ₃	23.3, CH ₃	28.7, CH ₃	17.1, CH ₃	24.3, CH ₃	24.0, CH ₃	23.3, CH ₃	19.9, CH ₃	17.4, CH ₃
17'	142.5, CH	145.8, CH	141.2, CH	147.5, CH	143.4, CH	146.7, CH	145.8, CH	141.9, CH	141.9, CH

Position	1	2	3	4	5	6	7	8	9
18'	114.5, CH ₂	112.0, CH ₂	114.2, CH ₂	111.6, CH ₂	112.2, CH ₂	111.7, CH ₂	111.1, CH ₂	111.8, CH ₂	112.4, CH ₂
OCH ₃						55.1	56.8		

Compound **8** was also isolated as yellowish oils with $[\alpha]_{25}^D -20.0$, and had a molecular formula of $C_{36}H_{46}O_3$ according to HRESIMS at m/z 525.3367 $[M - H]^-$ (calcd for $C_{36}H_{45}O_3$, 525.3369). The IR spectrum of **8** showed absorption bands at 3395, 1615, 1588, 1516, 1456, 1267 and 1010 cm^{-1} ascribable to hydroxyl group and ether functions and an aromatic ring. Its NMR spectroscopic data (Tables 1 and 2) was consistent with those of a known bisbakuchiol A [20], except for the chemical shifts of B ring. A set of ABX type NMR signals had disappeared in bisbakuchiol A, whereas a set of A_2B_2 type NMR signals appeared at δ_H 7.19 (2H, br d, $J = 8.6$ Hz, H-2', 6') and 6.73 (2H, br d, $J = 8.6$ Hz, H-3', 5') in compound **8**. The configuration of **8** was elucidated through NOESY experiments (Fig. 5), where correlations between H-8' at δ_H 3.97, and 16'-CH₃ at δ_H 0.62 suggested their same β -orientation. The coupling constant ($J = 7.3$ Hz) between H-7' and H-8' confirmed a *trans* configuration of the two methine protons of the dioxane ring [20]. Thus, the configuration of **8**, named bisbakuchiol T, was established as 9*S*,7'*S*,8'*S*,9'*S*, which was supported by comparison of the calculated and experimental ECD curves (Fig. 6).

Compound **9** was isolated as yellowish oils with $[\alpha]_{25}^D + 10.0$, and possessed the same molecular formula, $C_{36}H_{46}O_3$, as **8** according to the HRESIMS data (m/z 525.3371 $[M - H]^-$). The ¹H NMR and ¹³C NMR spectral data (Tables 1 and 2) of **9** were quite superimposable with those of compound **8**, which clearly indicated the same skeleton as that of **8**. Likely, NOE correlations between H-7' at δ_H 4.91 and 16'-CH₃ at δ_H 1.07, and the coupling constant ($J = 6.1$ Hz) between H-7' and H-8', indicated that the configuration of **9** was 9*S*,7'*R*,8'*R*,9'*S*, which was consistent with ECD data (Fig. 6). Therefore, the structure of compound **9**, named bisbakuchiol U, was established as shown in Fig. 1.

Compound **10** was also isolated as yellowish oils. Its HRESIMS data exhibited a sodium adduct ion at m/z 445.3080 $[M + Na]^+$, establishing the molecular formula as $C_{29}H_{42}O_2$. Comparison of ¹H and ¹³C NMR spectra of **10** (Table 3) and known bakuchiol, a side chain (3-ethenyl-3,7-dimethyl-1,6-octadienyl) and a *p*-disubstituted benzene ring of **10** were identical to that of bakuchiol. In addition, the COSY, HSQC and HMBC correlations showed the presence of 2-ethenyl-2-methyl-5-isopropanol-cyclopentan-1-ol (6-ethenyl-6-methyl-4-isopropanol-cyclopentan-5-ol) substituted group in **10**. Comparison of the ¹³C NMR spectrum of **10** with those of bakuchiol, the chemical shifts of C-3 and C-5 in **10** were shifted downfield to δ_C 124.5, suggesting that this substituted group was connected to C-4 of bakuchiol moiety by an ether linkage. The relative configuration was mainly assigned by NOESY spectrum. Furthermore, the signals of H-4' at δ_H 2.31 and H-5' at δ_H 4.01 showed an NOE correlation, whereas H-4' or H-5' and 11'-CH₃ no showed the NOE correlation in its the NOESY correlation, confirmed that both H-4' and H-5' were α -

oriented. Therefore, the structure of compound **10**, named bakuchiol ether A, was defined as shown in Fig. 1.

Compound **11** showed a molecular formula of $C_{33}H_{48}O_2$ on the basis of the HRESIMS ion at m/z 477.3713 $[M + H]^+$. Compared with the NMR data (Table 3) of compound **10**, a side chain (3-ethenyl-3,7-dimethyl-1,6-octadienyl) and a *p*-disubstituted benzene ring in **11** were identical to that of compound **10**. In addition, the COSY, HSQC and HMBC correlations in **11** showed the presence of clovane-2 β ,9 α -diol [21, 22] moiety with the exception of the resonances of C-1', C-2' to downfield shifts and C-3' and C-4' to highfield shifts. In the key HMBC spectrum (Fig. 4), correlations between H-2' at δ_H 4.24 and C-4 at δ_C 158.2 (s) revealed that C-4 of bakuchiol moiety was connected to C-2' of clovane-2 β ,9 α -diol moiety by an ether linkage. Therefore, the structure of compound **11**, named bakuchiol ether B, was defined as shown in Fig. 1.

Compound **12** was isolated as yellowish oils with $[\alpha]_{25}^D + 30.0$. It showed a molecular formula of $C_{33}H_{48}O_2$. The COSY, HSQC and HMBC correlations showed the presences of one set of the bakuchiol signals as in compound **12** and one set of the caryolane-1,9 β -diol signals [22]. Comparison of the ^{13}C NMR spectrum of **12** with those of bakuchiol, the chemical shifts of C-3 and C-5 were shifted downfield to δ_C 121.6 and the chemical shifts of C-1' was shifted downfield to δ_C 80.2 in **12**, suggesting that C-1' of this caryolane-1,9 β -diol moiety was connected to C-4 of bakuchiol moiety by an ether linkage. Therefore, the structure of compound **12**, named bakuchiol ether C, was defined as shown in Fig. 1.

When the quaternary carbon from the other unit was connected to bakuchiol unit by C–O–C₄, the chemical shifts of C-3 and C-5 would shift downfield (from 115 to 121 or 123 ppm) as shown in compounds **1**, **6**, **7**, **10**, **12**, **15**, **16** and **17**. Whereas, the link by CH–O–C₄ would not result in changes of δ_C at C-3 and C-5 as shown in compounds **3**, **4**, **5** and **11**. Therefore, we could infer the connection position of the dimers by the carbon chemical shifts of C-3/5 in bakuchiol unit.

Table 3

¹H NMR (400 MHz, CDCl₃; δ_{H} , *J* in Hz) data and ¹³C NMR (100 MHz, CDCl₃) data for compounds **10–12**.

Position	10		11		12	
	δ_{H} (<i>J</i> in Hz)	δ_{C}	δ_{H} (<i>J</i> in Hz)	δ_{C}	δ_{H} (<i>J</i> in Hz)	δ_{C}
1		134.9, C		130.3, C		131.4, C
2	7.27 (d, 8.6)	126.6, CH	7.25 (d, 8.7)	127.1, CH	7.20 (d, 8.7)	126.4, CH
3	6.93 (d, 8.6)	124.5, CH	6.82 (d, 8.7)	115.9, CH	6.79 (d, 8.7)	121.6, CH
4		153.5, C		158.2, C		154.7, C
5	6.93 (d, 8.6)	124.5, CH	6.82 (d, 8.7)	115.9, CH	6.79 (d, 8.7)	121.6, CH
6	7.27 (d, 8.6)	126.6, CH	7.25 (d, 8.7)	127.1, CH	7.20 (d, 8.7)	126.4, CH
7	6.28 (d, 16.3)	126.5, CH	6.25 (d, 16.2)	126.6, CH	6.25 (d, 16.3)	126.7, CH
8	6.12 (d, 16.3)	137.1, CH	6.04 (d, 16.2)	135.5, CH	6.06 (d, 16.3)	136.0, CH
9		42.6, C		42.5, C		42.5, C
10	1.49 (m)	41.2, CH ₂	1.49 (m)	41.3, CH ₂	1.49 (m)	41.3, CH ₂
11	1.94 (m)	23.2, CH ₂	1.95 (m)	23.2, CH ₂	1.95 (m)	23.2, CH ₂
12	5.12 (m)	124.8, CH	5.11 (br t, 7.1)	124.8, CH	5.11 (m)	124.8, CH
13		131.3, C		131.2, C		131.3, C
14	1.58 (s)	17.7, CH ₃	1.57 (s)	17.6, CH ₃	1.58 (s)	17.7, CH ₃
15	1.67 (s)	25.7, CH ₃	1.67 (s)	25.7, CH ₃	1.67 (s)	25.7, CH ₃
16	1.20 (s)	23.3, CH ₃	1.19 (s)	23.4, CH ₃	1.19 (s)	23.4, CH ₃

Position	10		11		12	
	δ_H (J in Hz)	δ_C	δ_H (J in Hz)	δ_C	δ_H (J in Hz)	δ_C
17	5.88 (dd, 17.4, 10.8)	145.8, CH	5.88 (dd, 17.4, 10.7)	146.1, CH	5.87 (dd, 17.4, 10.7)	146.0, CH
18a	5.10 (dd, 17.4, 1.3)	111.9, CH ₂	5.01 (dd, 17.4, 1.3)	111.8, CH ₂	5.01 (dd, 17.4, 1.3)	111.9, CH ₂
18b	5.04 (dd, 10.8, 1.3)		5.03 (dd, 10.7, 1.3)		5.03 (dd, 10.7, 1.3)	
1'	1.25 (s),	21.8, CH ₃		45.3, C		80.2, C
2'		84.1, C	4.24 (dd, 8.3, 5.4)	86.2, CH	2.35 (ddd, 11.7, 9.1, 8.6')	40.5, CH
3'	1.26 (s)	26.3, CH ₃	1.87 (dd, 12.9, 5.4), 1.65(m)	44.0, CH ₂	1.86 (dd, 9.1, 6.1), 1.72 (dd, 9.1, 8.6)	30.7, CH ₂
4'	2.31 (m)	53.7, CH		38.3, C		34.7, C
5'	4.01 (d, 9.0)	79.8, CH	1.58 (br d, 14.8)	50.1, CH	2.04 (ddd, 11.7, 9.1, 6.1)	44.9, CH
6'		47.8, C	1.39 (m), 1.49 (m)	20.9, CH ₂	1.41 (m), 1.53 (m)	21.3, CH ₂
7'	1.61 (m), 1.52 (m)	35.1, CH ₂	1.38 (m), 1.16 (m)	33.2, CH ₂	1.50 (m), 1.19 (m)	36.1, CH ₂
8'	1.95 (m), 1.49 (m)	22.8, CH ₂		34.7, C		39.2, C
9'	5.95 (dd, 17.6, 10.8)	146.7, CH	3.34 (br t, 2.6)	75.0, CH	3.50 (t, 4.7)	71.8, CH
10'a	5.03 (dd, 10.8, 1.3)	112.0, CH ₂	2.03 (m),	27.2, CH ₂	2.01 (dddd, 15.5, 12.5, 5.5, 3.0)	28.3, CH ₂
10'b	5.02 (dd, 17.6, 1.3)		1.80 (dd, 14.1, 5.1)		1.78 (ddt, 15.5, 5.5, 3.0)	
11'a	1.10 (s)	17.2, CH ₃	1.38 (m)	26.7, CH ₂	1.71 (m)	37.5, CH ₂
11'b			1.06 (m)			
12'			1.56 (br s), 1.02 (br s)	36.0, CH ₂	1.64 (d, 16.4), 1.49 (d, 16.4)	42.1, CH ₂

Position	10		11		12	
	δ_H (J in Hz)	δ_C	δ_H (J in Hz)	δ_C	δ_H (J in Hz)	δ_C
13'			0.94 (s)	25.7, CH ₃	1.01 (s)	20.9, CH ₃
14'			1.06 (s)	31.4, CH ₃	1.00 (s)	30.3, CH ₃
15'			0.95 (s)	28.4, CH ₃	0.92 (s)	26.4, CH ₃

NO, an unstable biological free radical, comes of *L*-arginine under the action of constitutive NO synthase (cNOS) and inducible NO synthase (iNOS). NO functions as a signaling molecule participating in neurotransmission and vasodilation. However, overproduction of NO is involved in inflammatory diseases, which can be treated by NO inhibitor. Compounds **1–17** (3.125–50 μ M) were assay inhibition effect on NO production in LPS-stimulated RAW264.7 macrophages using the Griess reaction [14]. The MTT tests demonstrated that compound **4** showed cytotoxicity at the concentration of 50 μ M, whereas other compounds were not cytotoxic. L-NIL, a selective inhibitor of iNOS, was used for the positive control. Compound **1** exhibited significant inhibition of NO production with IC₅₀ value at the concentration of 11.47 ± 1.57 μ M, which showed no significant difference with that of L-NIL (10.29 ± 1.10 μ M). Compounds **2, 3, 10–12, 16** and **17** exhibited moderate inhibitory activity with IC₅₀ values at the range of 15.98–27.80 μ M. The IC₅₀ values of the other compounds were more than 50 μ M, and they were ineffective against NO production.

Table 5
Inhibition of **1–3**, **10–12** and **16–17** on NO production.

Compound	IC ₅₀ (μM)
1	11.47 ± 1.57
2	23.52 ± 1.82
3	21.43 ± 2.04
10	27.80 ± 1.18
11	26.86 ± 1.05
12	23.54 ± 0.82
16	15.98 ± 2.30
17	24.93 ± 1.13
L-NIL	10.29 ± 1.10

4. Discussion

In our previous researches, we have obtained fourteen meroterpenoids and seventeen heterodimers of bakuchiol and evaluated their cytotoxicity [11, 12]. Further investigation on the cHE extract brought about twelve unrepresented bakuchiol dimmers and their NO inhibition activities were studied. In sum, Structural changes in bakuchiol increases structural and bioactive diversity of constituents from *Psoraleae Fructus*. And a new skeleton compound (**1**) was isolated and the compound exhibited significant NO inhibition activities.

5. Conclusion

Seventeen bakuchiol dimers (**1–17**), including 12 undescribed dimers and 5 known compounds, were isolated from the fruits of *Psoralea corylifolia* L. and their structure were identified by spectral methods and X-ray single-crystal diffraction. Bisbakuchiol M (**1**), whose other bakuchiol unit was cyclized to form a 6/6/5 tricyclic system, was a new skeleton compound. And the plausible biosynthetic pathway of bisbakuchiol M was proposed. Their inhibition on NO production in LPS-stimulated RAW264.7 macrophages were evaluated by the Griess reaction. Compounds **2**, **3**, **10–12**, **16** and **17** exhibited inhibitory activities, and the inhibition of compound **1** was equal to that of L-NIL, a positive control. These findings suggested that *Psoraleae Fructus* provided natural anti-inflammatory constituents and bisbakuchiol M had the potential to be novel NO inhibitor.

Abbreviations

TCM: Traditional Chinese medicine; NO: nitric oxide; IC₅₀: half maximal inhibitory concentration; CC: open column chromatography; TLC: thin layer chromatography; RP-SP-HPLC: reversed phase semi-preparative HPLC; PE: petroleum ether; cHE: cyclohexane; EtOAc: ethyl acetate; DMEM: Dulbecco's modified Eagle's medium; FBS: fetal bovine serum; CHCl₃: chloroform; BuOH: normal-butanol; MTT: 3-(4,5-Dimethyl-2-thiazolyl)-2,5-diphenyl-2H-tetrazolium bromide; LPS: lipopolysaccharide; DMSO: dimethylsulfoxide; L-NIL: L-N⁶-(1-iminoethyl)-lysine.

Declarations

Author's contributions

XWY and YTZ designed the experiments. QXX and QL were responsible for isolation experiment. QXX finished biological activity assay. LL performed LC/MS analysis. XWY and QXX wrote the manuscript. All authors read and approved the final manuscript.

Acknowledgements

Not applicable.

Funding

This work was supported by the National Natural Science Foundation of China (81773865).

Availability of data and materials

All data included in this article are available from the corresponding author upon request.

Consent for publication

All authors have provided consent for publication in the journal of Chinese Medicine.

Conflicts of Interest

The authors declare no conflict of interest.

References

1. Ai TM. Medicinal Flora of China, Peking University Press, Beijing, 2016; vol. **5**, p. 585–588.
2. Chinese Pharmacopoeia Commission. Pharmacopoeia of the People's Republic of China, Chinese Medical Science and Technology Press, Beijing, 2015, vol. 1, p. 187–188.
3. Chino M, Sato K, Yamazaki T and Maitani T. Constituent of natural food additive hokosshi extract and an analytical method for the additive in foods. *Shokuhin Eiseigaku Zasshi*. 2002; 43(6):352–355.

4. Chopra B, Dhingra AK and Dhar KL, *Psoralea corylifolia* L. (Buguchi) - folklore to modern evidence: review. *Fitoterapia*. 2013;90:44–56.
5. Zhang XN, Zhao WW, Wang Y, Lu JJ and Chen XP. The Chemical Constituents and Bioactivities of *Psoralea corylifolia* Linn.: A Review. *Am. J. Chin. Med.* 2016;44(1):35–60.
6. Lim SH, Ha TY, Kim SR, Ahn J, Park HJ and Kim S, Ethanol extract of *Psoralea corylifolia* L. and its main constituent, bakuchiol, reduce bone loss in ovariectomised Sprague-Dawley rats. *Br. J. Nutr.* 2009;101(7):1031–1039.
7. Kim YJ, Lim HS, Lee J and Jeong SJ. Quantitative Analysis of *Psoralea corylifolia* Linne and its Neuroprotective and Anti-Neuroinflammatory Effects in HT22 Hippocampal Cells and BV-2 Microglia. *Molecules*. 2016;21(8):1076.
8. Lin X, Li BB, Zhang L, Li HZ, Meng X, Jiang YY, Lee HS and Cui L. Four new compounds isolated from *Psoralea corylifolia* and their diacylglycerol acyltransferase (DGAT) inhibitory activity. *Fitoterapia*. 2018;128:130–134.
9. Sun NJ, Woo SH, Cassady JM and Snapka RM. DNA polymerase and topoisomerase II inhibitors from *Psoralea corylifolia*. *J. Nat. Prod.* 1998;61(3):362–366.
10. Gao HTY, Lang GZ, Zang YD, Ma J, Yang JZ, Ye F, Tian JY, Gao PP, Li CJ and Zhang DM. Bioactive monoterpene phenol dimers from the fruits of *Psoralea corylifolia* L. *Bioorg Chem.* 2021;112:104924.
11. Xu QX, Zhang YB, Liu XY, Xu W and Yang XW. Cytotoxic heterodimers of meroterpene phenol from the fruits of *Psoralea corylifolia*. *Phytochemistry*. 2020;176:112394.
12. Xu QX, Xu Wand Yang XW. Meroterpenoids from the fruits of *Psoralea corylifolia*. *Tetrahedron*. 2020;76:131343.
13. MosMann T. Rapid colorimetric assay for cellular growth and survival: application to proliferation and cytotoxicity assays. *J. Immunol. Methods*. 1983;65:55–63.
14. Cao GY, Xu W, Yang XW, Gonzalez FJ and Li F. New neolignans from the seeds of *Myristica fragrans* that inhibit nitric oxide production. *Food Chem.* 2015;173:231–237.
15. Labbe C, Faini F, Coll J and Connolly JD. Bakuchiol derivatives from the leaves of *Psoralea glandulosa*. *Phytochemistry*. 1996;42(5):1299–1303.
16. Xiao GD, Li XK, Wu T, Cheng ZH, Tang QJ and Zhang T. Isolation of a new meroterpene and inhibitors of nitric oxide production from *Psoralea corylifolia* fruits guided by TLC bioautography. *Fitoterapia*. 2012;83(8):1553–1557.
17. Banerji A and Chintalwar GJ. Biosynthesis of bakuchiol, a meroterpene from *Psoralea corylifolia*. *Phytochemistry*. 1983;22(9):1945–1947.
18. Takano S, Shimazaki Y and Ogasawara K. Enantiocontrolled synthesis of natural (+)-bakuchiol. *Tetrahedron Lett.* 1990;31:3325–3326.
19. Yin S, Fan CQ, Dong L and Yue JM. Psoracorylifols A–E, five novel compounds with activity against *Helicobacter pylori* from seeds of *Psoralea corylifolia*. *Tetrahedron*. 2006;62:2569–2575.

20. Wu CZ, Cai XF, Dat NT, Hong SS, Han AR, Seo EK, Hwang BY, Nan JX, Lee D and Lee JJ. Bisbakuchiols A and B, novel dimeric meroterpenoids from *Psoralea corylifolia*. *Tetrahedron Lett.* 2007;48(50):8861–8864.
21. Wang AX, Zhang Q, and Jia ZJ. A new furobenzopyranone and other constituents from *Anaphalis lactea*. *Pharmazie.* 2004;59(10):807–811.
22. Heymann H, Tezuka Y, Kikuchi T, and Supriyatna S. Constituents of *Sindora sumatrana* MIQ. III. New trans-clerodane diterpenoids from the dried pods. *Chem. Pharm. Bull.* 1994;42(6):138–146.

Figures

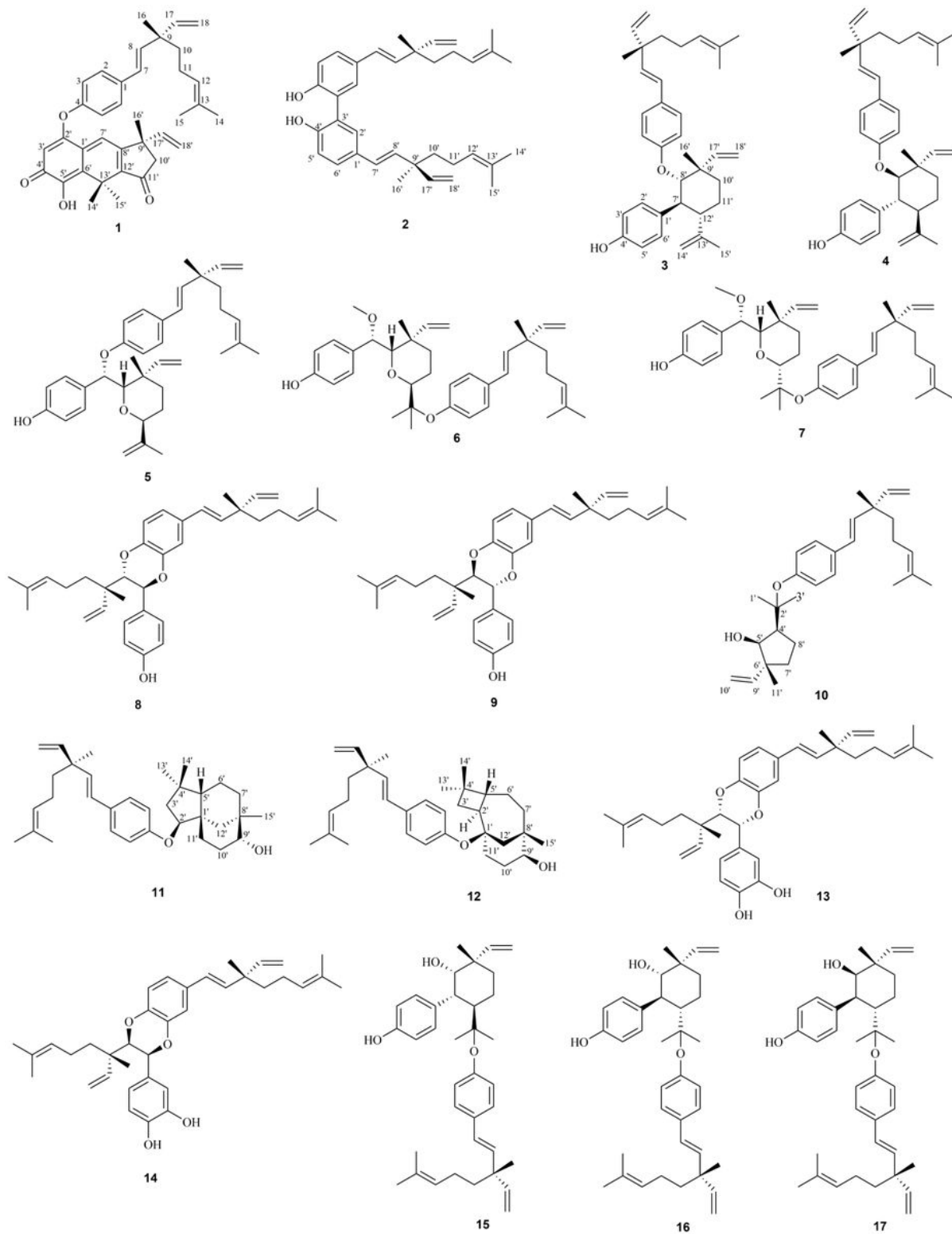


Figure 1

Structures of compounds 1–17.

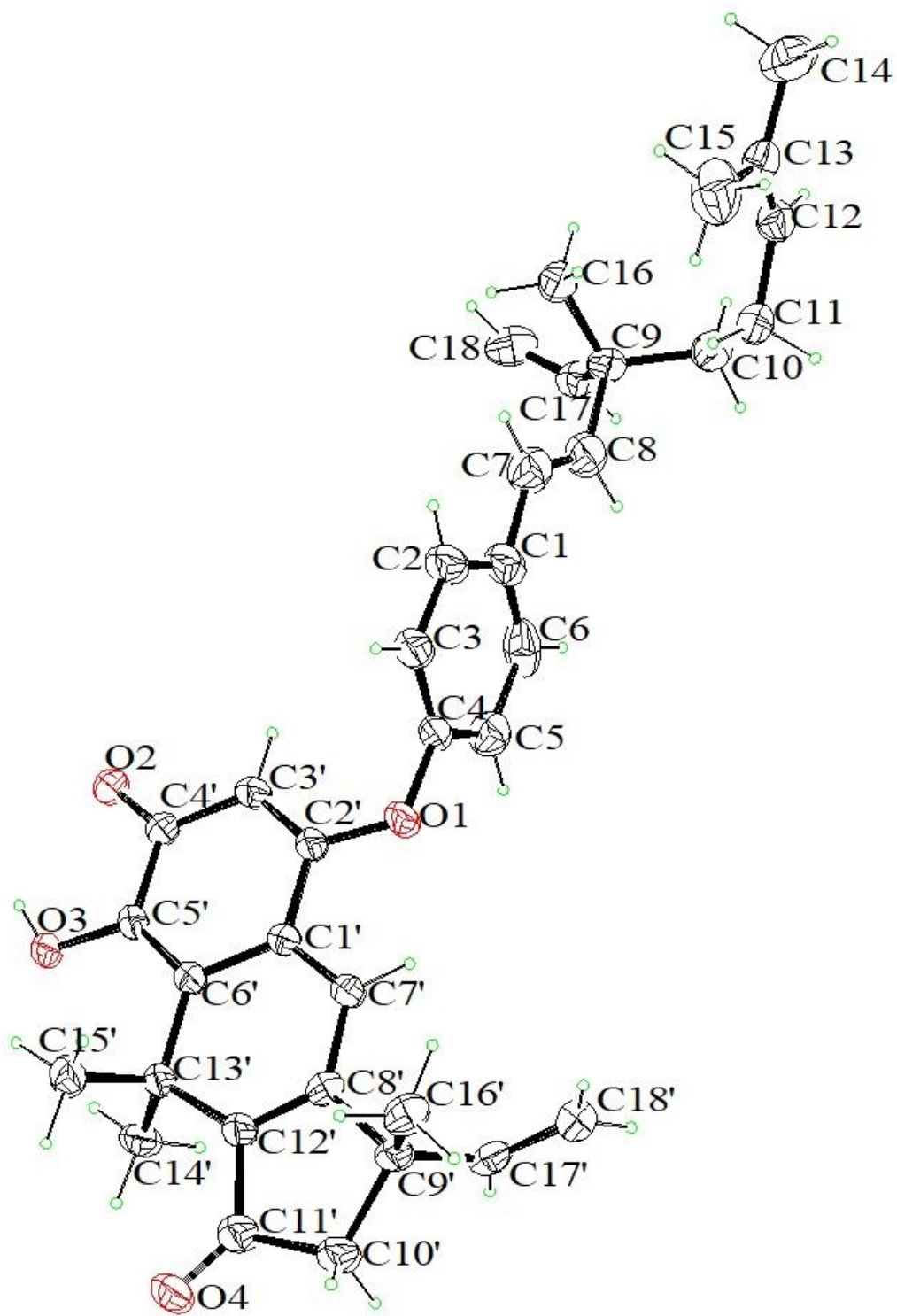


Figure 2

X-ray ORTEP drawings of 1.

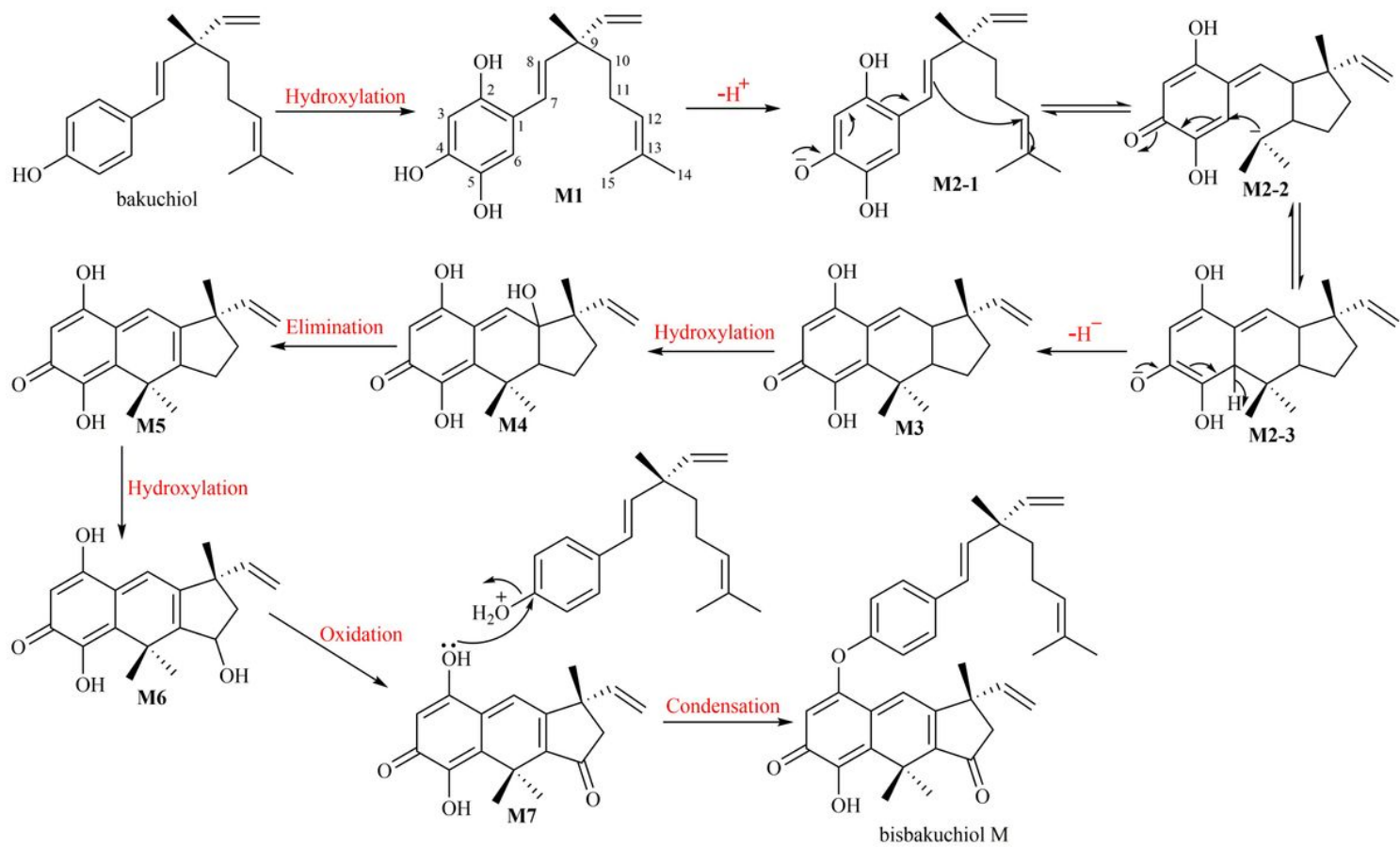


Figure 3

Plausible biogenetic pathway of 1.

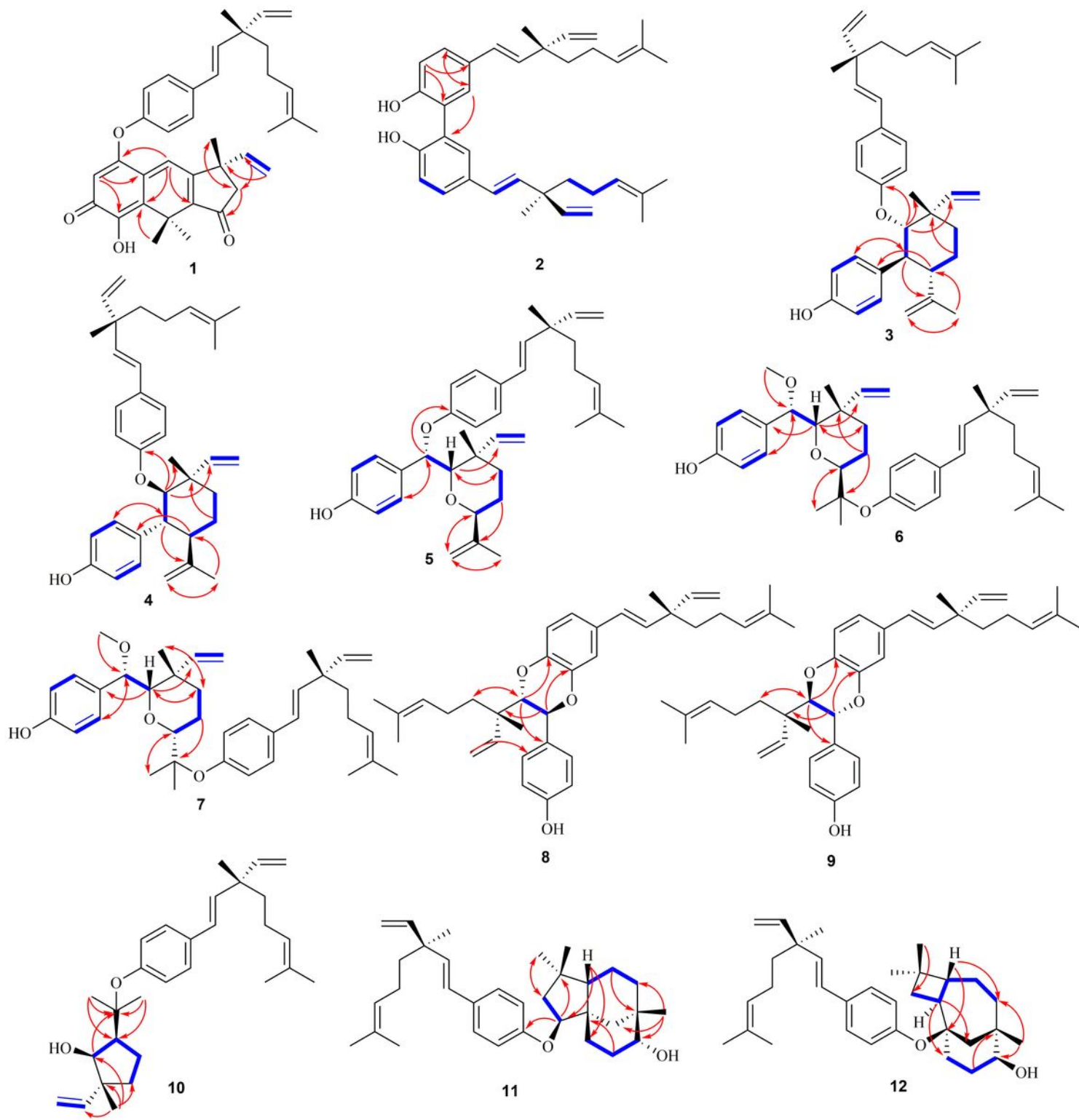


Figure 4

Key ^1H - ^1H COSY and HMBC correlations of 1-12.

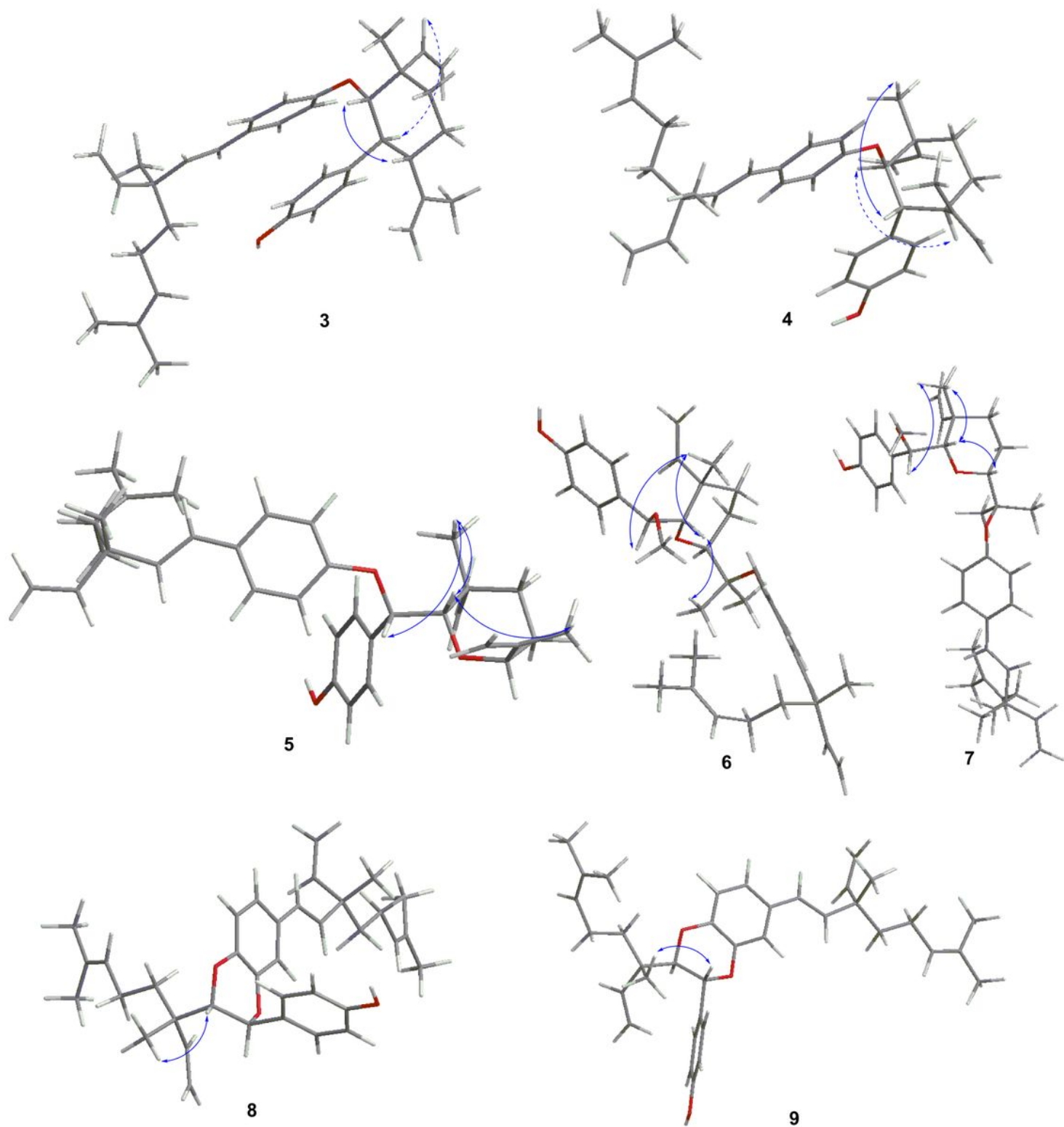


Figure 5

Key NOESY correlations of 3-9.

Supplementary Files

This is a list of supplementary files associated with this preprint. Click to download.

- [Supplementarymaterial.docx](#)